A Review of Li-ion Battery Equivalent Circuit Models

Xiaoqiang Zhang[†], Weiping Zhang, and Geyang Lei
North China University of Technology, Beijing 100144, China

Batteries are critical components of electric vehicles and energy storage systems. The connection of a battery to the power grid for charge and discharge greatly affects energy storage. Therefore, an accurate and easy-to-observe battery model should be established to achieve systematic design, simulation, and SOC (state of charge) estimations. In this review, several equivalent circuit models of representative significance are explained, and their respective advantages and disadvantages are compared to determine and outline their reasonable applications to Li-ion batteries. Numerous commonly used model parameter identification principles are summarized as well, and basic model verification methods are briefly introduced for the convenient use of such models.

Keywords: Li-ion battery, Equivalent circuit model, Parameter identification, Model verification

1. INTRODUCTION

In recent years, Li-ion batteries have become increasingly used for various applications. As such, many studies have comprehensively analyzed Li-ion battery models based on the demand for Li-ion battery applications. A Li-ion battery model demonstrates the mathematical relationship between the influential elements of Li-ion batteries and their working characteristics, including voltage, current, power, SOC (state of charge), temperature, internal resistance, internal voltage, operation cycles, and self-discharge. Reference [1] summarizes the considerable research on Li-ion battery models and divides such models into four categories, namely, electrochemical, thermal, coupling, and performance models. The electrochemical model is based on electrochemical theories and describes the reaction that occurs in a Li-ion battery. The thermal model looks into the heat building and transmission of Li-ion batteries. The coupling model describes the interactive effects of the electrochemical process as well as the heat building and transmission of such batteries. Finally, the performance model describes the external features of Li-ion batteries during operation. Among all these models, the performance model can be used easily and has diverse structures.

The equivalent circuit model is a Li-ion battery performance model used to simulate the dynamic characteristics of a Li-ion battery using resistance, capacitance, voltage source, and other circuit components to form a circuit. This model has been widely used in studies related to electric vehicles and energy storage systems. The implications of investigating Li-ion battery models for electric vehicles and energy storage systems are apparent in the simulation of such vehicles and systems as well as in the proper administration of SOC estimation and Li-ion battery management. Studies on Li-ion battery models involve analysis from the perspectives of Li-ion battery usage and management more than the design and production. As such, the equivalent circuit model is generally used in analyses through the application of circuit and mathematical methods and has therefore become the most widely adopted Li-ion battery model. Reference [2] introduces several typical equivalent circuit models and presents a universal battery model. Reference [3] develops a modified equivalent circuit model based on the typical models.

In this review, numerous Li-ion battery equivalent circuit models are introduced in detail along with their respective advantages and disadvantages. In addition, several commonly used model parameter identification methods are analyzed, and some disputable ones are even briefly explained. Finally, some of the commonly adopted verification methods are discussed.

[†] Author to whom all correspondence should be addressed:
E-mail: zxq@ncut.edu.cn

2. ANALYSIS OF THE COMMONLY ADOPTED Li-ion BATTERY EQUIVALENT CIRCUIT MODELS

Battery equivalent circuit models are used to describe the working characteristics of Li-ion batteries through a circuit network based on principles about how the battery works. As such, these models can be used to analyze further diversified batteries. Researchers have developed many Li-ion battery equivalent circuit models to meet the demands for simulative technologies. Reference [4] divides the existing methods used to establish equivalent circuit models into two categories of time and frequency domain analysis models. The time domain analysis model mainly uses Li-ion battery voltage and current data, whereas the frequency domain analysis model primarily adopts the Nyquist and Bode diagrams measured with Li-ion battery impedance. The most commonly used equivalent circuit models are established through time domain analysis. This review is focused on the RC, PNGV, Thevenin, and modified Thevenin models [5].

2.1 RC model

An RC model is composed of two capacitances and three resistances as shown in Fig. 1 [6]. The large capacitance C_b describes the ability of the Li-ion battery to store electric charges, the small capacitance C_s represents the surface capacity and the diffusion effect of the Li-ion battery, R_t is the terminal resistance, R_s is the surface resistance, and R_e is the end resistance.
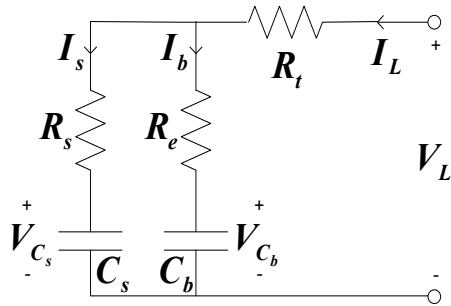

Fig. 1. RC model.

Voltages V_{Cb} and V_{Cs} at both ends of the two capacitances are the status variables, terminal current I_L is the input variable, and terminal voltage V_L is the output variable. Equation (1) is formulated based on Kirchhoff's law from which the RC model state space equation is deduced.

$$
\begin{bmatrix} \dot{V}_{C_b} \\ \dot{V}_{C_s} \end{bmatrix} = \begin{bmatrix} -\dfrac{1}{(R_e + R_s)C_b} & \dfrac{1}{(R_e + R_s)C_b} \\ \dfrac{1}{(R_e + R_s)C_s} & -\dfrac{1}{(R_e + R_s)C_s} \end{bmatrix} \begin{bmatrix} V_{C_b} \\ V_{C_s} \end{bmatrix} + \begin{bmatrix} \dfrac{R_s}{(R_e + R_s)C_b} \\ \dfrac{R_e}{(R_e + R_s)C_s} \end{bmatrix} I_L \quad (1)
$$
$$
V_L = \begin{bmatrix} \dfrac{R_s}{R_e + R_s} & \dfrac{R_e}{R_e + R_s} \end{bmatrix} \begin{bmatrix} V_{C_b} \\ V_{C_s} \end{bmatrix} + (\dfrac{R_e R_s}{R_e + R_s} + R_t)I_L
$$

Reference [6] establishes an extended Kalman filter with the RC model, and reference [7] uses the RC model to develop a sliding mode controller for Li-ion battery SOC estimation.

2.2 Thevenin model

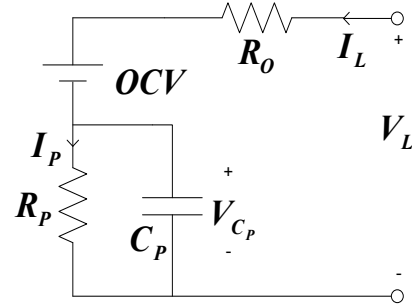The Thevenin model depicted in Fig. 2 is a commonly used

Fig. 2. Thevenin model.

model [4]. This model describes the Li-ion battery OCV (open circuit voltage) through an ideal voltage source and uses the series resistance R_O and an RC parallel network (RP and CP) to predict the response of the Li-ion battery to the instantaneous load at a certain SOC.

Voltage V_{Cp} at both ends of capacitance C_p is the state variable, terminal current I_L is the input variable, and terminal voltage V_L is the output variable. Equation (2) is then formulated based on Kirchhoff's law, from which the Thevenin model state-space equation is deduced.

$$
\dot{V}_{C_P} = -\frac{1}{R_P C_P} V_{C_P} + \frac{1}{C_P} I_L
$$
$$
V_L = V_{C_P} + R_O I_L + OCV
$$
$$(2)$$

Owing to its comparable simplicity and ability to meet the basic requirements for Li-ion battery, the Thevenin model has been extensively used. However, if the *OCV* does not change with SOC, the model can only be used to describe the temporary responses of the Li-ion battery at a certain SOC. Correspondingly, the model can neither be used to describe the steady voltage changes of Li-ion batteries nor to predict their operation duration. The model also fails to describe the relationship between the battery's *OCV* and SOC as well as to predict its operation duration and the charge and discharge management. Certain types of derivative circuits, such as capacitors, can be formed by adding some components to the circuit to attain improved simulation effects.

2.3 PNGV model

The PNGV model is obtained by adding a capacitor C_o to the Thevenin model as depicted in Fig. 3 [8]. This model is of distinct physical significance, with the ideal voltage source *OCV* indicating the Li-ion battery's OCV. Resistance R_O is the battery's ohmic internal resistance, resistance R_p is the polarization inter-
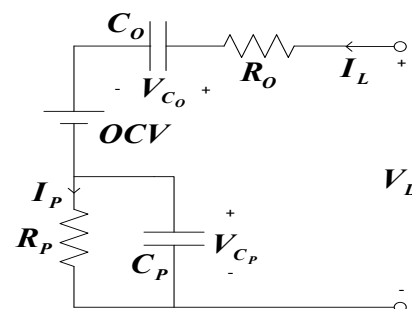

Fig. 3. PNGV model.

nal resistance, capacitance C_p is the polarization capacity, I_L is the load current, I_p is the polarization current, V_L is the terminal voltage, and capacitance C_o refers to the changes in *OCV* caused by the timely integration of load current I_L. When the Li-ion battery is in a charging or discharging state, the accumulation of current with time changes the SOC, which in turn further changes the battery's OCV, represented by voltage changes on the capacitor C_o. In this model, capacitance C_o not only represents the capacity of the Li-ion battery but also its direct current response, thereby compensating for the deficiencies of the Thevenin model.

Voltage V_{Co} at both ends of capacitance C_o and voltage V_{Cp} at both ends of capacitance C_p are the state variables, terminal current I_L is the input variable, and terminal voltage V_L is the output variable. Equation (3) is then developed based on Kirchhoff's law from which the PNGV model state-space equation is deduced.

$$\begin{bmatrix} \dot{V}_{C_o} \\ \dot{V}_{C_P} \end{bmatrix} = \begin{bmatrix} 0 & 0 \\ 0 & -\dfrac{1}{R_P C_P} \end{bmatrix} \begin{bmatrix} V_{C_o} \\ V_{C_P} \end{bmatrix} + \begin{bmatrix} \dfrac{1}{C_O} \\ \dfrac{1}{C_P} \end{bmatrix} I_L$$

$$V_L = \begin{bmatrix} 1 & 1 \end{bmatrix} \begin{bmatrix} V_{C_o} \\ V_{C_P} \end{bmatrix} + R_O I_L + OCV \tag{3}$$

The PNGV model is the Li-ion battery model introduced by the US PNGV and is significantly influenced by the Freedom CAR hybrid electric vehicles. Parameter identification experiments can easily be conducted using this model owing to its systematic parameter identification methods and comparatively high model accuracy. As such, this model is among the most frequently adopted models.

2.4 Modified thevenin model

The unipolar models of Li-ion batteries cannot always meet the dynamic performance requirements; thus, researchers have introduced many bipolar and multi-polar models [9]. Among these models, the modified thevenin model shown in Fig. 4 is frequently used. In this model, the ideal voltage source represents the *OCV* of the Li-ion battery, resistance R_O is the ohmic internal resistance, resistance R_e is the electrochemical polarization internal resistance, capacitance C_e is the electrochemical polarization capacitance, resistance R_c is the concentration polarization internal capacitance, capacitance C_c is the concentration polarization capacitance, V_{Ce} is the electrochemical polarization voltage, V_{Cc} is the concentration polarization voltage, I_L is the load current, and V_L is the terminal voltage.

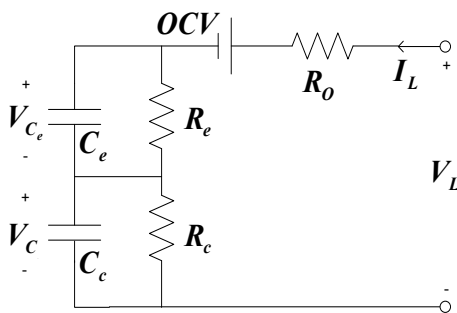The electrochemical polarization voltage V_{Ce} and the concen-

tration polarization voltage V_{Cc} are the state variables, terminal current I_L is the input variable, and terminal voltage V_L is the output variable. Equation (4) is drawn based on Kirchhoff's law from which the modified Thevenin model state-space equation is deduced.

$$\begin{bmatrix} \dot{V}_{C_e} \\ \dot{V}_{C_c} \end{bmatrix} = \begin{bmatrix} -\dfrac{1}{R_e C_e} & 0 \\ 0 & -\dfrac{1}{R_c C_c} \end{bmatrix} \begin{bmatrix} V_{C_e} \\ V_{C_c} \end{bmatrix} + \begin{bmatrix} \dfrac{1}{C_e} \\ \dfrac{1}{C_c} \end{bmatrix} I_L$$

$$V_L = \begin{bmatrix} 1 & 1 \end{bmatrix} \begin{bmatrix} V_{C_e} \\ V_{C_c} \end{bmatrix} + R_O I_L + OCV \tag{4}$$

The polarization of the modified Thevenin model includes the accurate demonstration of the dynamic characteristics of the battery. This model is increasingly used because of the increasing demands on Li-ion battery performance. However, similar to its original version, the modified Thevenin model fails to describe the changes in *OCV* caused by the timely integration of the load current I_L. If the *OCV* in the Thevenin model is a variable, then the Li-ion battery *OCV-SOC* relationship equivalence can replace capacitance C_o in the PNGV model. In spite of their deficiencies, the Thevenin model and its modified version are still of great practical significance.

2.5 Other models

Reference [10] introduces the CPE (constant phase element) in detail. This equivalent electrical circuit component can be used to describe the impedance-based equivalent circuit model. CPE impedance has multiple definitions, one of which is expressed below.

$$Z_{CPE} = \frac{1}{T(j\omega)^\phi} \tag{5}$$

Where T is a constant, and Φ is related to the rotation angles of the pure capacitive lines on the complex planes. In general cases, $\Phi=1$ represents a pure capacitance, $\Phi=0.5$ represents the infinite Warburg impedance, $\Phi=0$ denotes a pure impedance, and $\Phi=-1$ indicates a pure inductance.

Reference [11] establishes an impedance-based universal equivalent circuit model, which is shown in Fig. 5. In this model, L is the parasitic inductance, R_O is the ohmic internal resistance, C_{DL} (CPE) represents the double-electrode layers, R_{CT} is the charge transfer, and Z_W (CPE) is the Warburg impedance representing diffusion.

Such an impedance-based universal equivalent circuit model is only applicable to situations in which the frequency is already fixed or known because of difficulties in impedance measurement or in the transformation from the frequency to the time domain.

Reference [9] introduces and compares several second- and third-order equivalent circuit models, whose working principles are similar to those of the modified Thevenin model. Reference
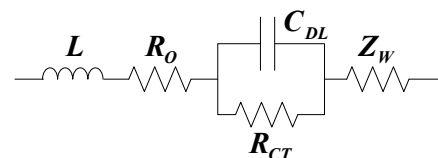

Fig. 4. Modified thevenin model.

Fig. 5. Impedance-based universal equivalent vircuit model.

314

Trans. Electr. Electron. Mater. 17(6) 311 (2016): X. Zhang *et al.*

[12] proposes a Randle equivalent circuit model. This model divides the polarization resistance of the Thevenin model into two and describes their functions respectively based on their physical significance. Reference [13] presents the Massimo Ceraolo equivalent circuit model, a modified Thevenin model with a self-discharge resistance similar to the GNL model in reference [2].

3. MODEL PARAMETER IDENTIFICATION

The existing Li-ion battery model parameter identification methods can be divided roughly into two categories. The methods that belong to the first category determine the model parameters through calculation equations and are applicable only to specific models. By contrast, the methods that belong to the second category obtain the model parameters through data fitting and are appropriate for most models. Nonetheless, both methods can only be adopted through auxiliary experiments. This review explains the three model identification methods.

3.1 Identification method I

Reference [6] explains the calculation of RC models in detail. The mechanism is explained in the succeeding paragraphs.

First, capacitance C_b should be calculated. The energy stored in capacitance C_b can be determined through OCV at 0%SOC and 100%SOC and is equal to the Li-ion battery's rated capacity Q_{rated}.

$$C_b = \frac{2Q_{rated}V_{100\%SOC}}{V_{100\%SOC}^2 - V_{0\%SOC}^2} \tag{6}$$

Second, capacitance C_s should be identified. The pulse discharge experiment shown in Fig. 6 is conducted; it can be assumed to be approximately $V_1 = V_3 + (V_4 - V_3)(1 - e^{t/\tau})$ at empty load, and the time constant τ can be deduced. Given the time constant $\tau = (R_e + R_s)C_s$.
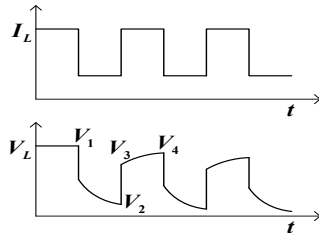

Fig. 6. Discharge pulse experiment diagram.

$$C_s = \frac{\tau}{R_e + R_s} \tag{7}$$

Third, resistances R_t, R_e, and R_s should be estimated. R_e is assumed to be equal to R_s and comprises 80% of the total resistance. R_t, R_e, and R_s can then be calculated from the measured total resistance.

The identification method explained in the preceding paragraph is comparatively rough but can meet the ordinary demands.

3.2 Identification method II

Reference [8] details the parameter identification methods

employed in PNGV models, whose working principles are explained below.

The first principle is to conduct HPPC experiments. Time t_k, terminal current $I_{L,k}$, and terminal voltage $V_{L,k}$ can be obtained through equal interval SOC HPPC experiments. The integral $(\Sigma I_L \Delta t)_k$ of the terminal current on time can be calculated with equation (8). This integral refers to changes in the charges in comparison with their initial states.

$$(\Sigma I_L \Delta t)_k = (\Sigma I_L \Delta t)_{k-1} + \frac{I_{L,k} + I_{L,k-1}}{2} \cdot \Delta t \tag{8}$$

The second principle is to conduct multivariate linear regression analysis. The polarization time constant τ is estimated, and the polarization current $I_{P,K}$ is calculated with equation (9). $(\Sigma I_L \Delta t)_k$, $I_{L,K}$ and $I_{P,K}$ are the independent variables, and $V_{L,K}$ is the dependent variable. The multivariate linear regression analysis is conducted based on equation (10), from which the model parameters OCV, $1/C_o$, R_o, and R_p as well as the fitting determination coefficient r^2 are deduced.

$$I_{P,k} = (1 - \frac{1 - e^{-\Delta t/\tau}}{\Delta t/\tau}) \cdot I_{L,k} +$$
$$(\frac{1 - e^{-\Delta t/\tau}}{\Delta t/\tau} - e^{-\Delta t/\tau}) \cdot I_{L,k-1} + e^{-\Delta t/\tau} \cdot I_{P,k-1} \tag{9}$$

$$V_{L,k} = OCV + (1/C_O) \cdot (\Sigma I_L \Delta t)_k$$
$$+ R_O \cdot I_{L,k} + R_P \cdot I_{P,k} \tag{10}$$

The last principle is to determine the model parameters. The polarization time constant τ is changed to repeat the above processes until the maximum fitting determination coefficient r^2 is obtained, from which model parameters OCV, C_o, R_o, R_p and C are deduced at the τ value.

This identification method is applicable to PNGV models, Thevenin models, modified Thevenin models, and other polarization models.

3.3 Identification method III

Reference [13] introduces the identification of model parameters through z-transform methods, whose working principles are stipulated in the subsequent paragraphs.

First, the s domain equation should be acquired. For the PNGV model shown in Fig. 2, OCV is a constant, and a new terminal voltage $V_L' = V_L - OCV$ can be obtained when the constant is rid of the circuit. The s equation of the circuit is

$$V_L'(s) = (\frac{R_P}{sR_PC_P} + \frac{1}{sC_O} + R_O) \times I_L(s) \tag{11}$$

Second, the discrete s domain equation should be obtained. Conducting z-transform on the obtained s domain equation can yield the following discrete difference equation:

$$v'(k) = av'(k-1) + bv'(k-2)$$
$$+ ci(k) + di(k-1) + ei(k-2) \tag{12}$$

where, $a = 1 + e^{-\theta T}$, $b = -e^{-\theta T}$, $c = -R_O$, $d = -2R_P - (1 - e^{-\theta T})(R_O + R_P) - T/C_O$, $e = R_P - (1 - e^{-\theta T})(R_O + R_P)e^{-\theta T} + e^{-\theta T}T/C_O$, $\theta = 1/R_PC_P$, and T is the

sampling time.

Finally, parameters *a, b, c, d*, and *e* should be identified, and the model parameters should be calculated. Equation (12) can then be rewritten as

$$
\begin{aligned}
v'(k) &= \varphi^T(k)\lambda \\
\varphi^T(k) &= \begin{bmatrix} v'(k-1) & v'(k-2) & i(k) & i(k-1) & i(k-2) \end{bmatrix} \\
\lambda &= \begin{bmatrix} a & b & c & d & e \end{bmatrix}^T
\end{aligned} \tag{13}
$$

The recursive least squares can be expressed as follows:

$$
\hat{\lambda}_{k+1} = \lambda_{k+1} + G_{k+1}\big[u_{k+1} - \varphi_{k+1}^T \lambda_k\big] \tag{14}
$$

where $G_{k+1} = \dfrac{P_k \varphi_{k+1}}{1 + \varphi_{k+1}^T P_k \varphi_{k+1}}$, and $P_{k+1} = P_k - G_{k+1}\varphi_{k+1}^T P_k$. After a,b,c,d,

and e are obtained with recursive least squares, the model parameters can be obtained through calculation based on known data.

Reference [14] also introduces the recursive least squares that have weighting factors, and as a supplement, describes some details for the application of the method.

3.4 Other identification methods

References [2] and [3] both determine the model's ohmic internal resistance by considering the circuit responses to the pulse charge and performing discharge experiments. These studies then fit the model parameters based on other circuit relationships using least square methods.

Reference [10] presents a CPE model parameter calculation method, and reference [15] uses small signal square waves to identify the time domain parameters of the CPE model.

Reference [12] proposes that the ohmic resistance of the Randle model performs a linear change along with the discharge, and the remaining two resistances have an exponential relationship with the discharge time. The model parameters are then identified through discharge experiments and nonlinear least square methods.

4. MODEL VERIFICATION

A model can be verified after it has been established for future application. One commonly adopted verification method [1] is to conduct the same tests with the Li-ion battery and the corresponding Li-ion battery model under the same conditions. The results of the Li-ion battery experiment should then be compared with the simulation results from the Li-ion battery model for evaluation taking into consideration the average error, mean square error, or other indexes.

Verification experiments can be classified into two, namely, steady state or dynamic experiments. In steady state experiments, different current levels are normally adopted for the charge or discharge process with a constant current. Contrarily, dynamic experiments are conducted using self-designed or typical verification cycles (e.g., FUDS, NEDC, and FTP-75)[16]. Driving cycles usually have requirements on velocity or power, and when a Li-ion battery experiment is conducted, the method provided in reference [17] can be followed to convert the velocity or power input into the current input.

The experiments require long durations for verification of model stability. The driving cycle experiments can be repeated

simply or designed as required. Reference [8] details various experiments for verifying Li-ion battery performance.

5. CONCLUSION

Considering the increasingly extensive application of Li-ion batteries, this review collects and presents the existing equivalent circuit models. In particular, the models are thoroughly described, and their respective advantages and disadvantages are analyzed. In addition, several commonly adopted model parameter identification methods are discussed, and the basic methods and frequently used experiments for model verification are briefly explained. In recent years, the requirements on Li-ion batteries brought about by electric vehicles and energy storage systems have drawn the attention of researchers to focus on Li-ion battery circuit models. The model establishment process for various Li-ion battery circuit models can be summarized as applicability analysis, circuit model selection, parameter identification, and model verification. A universal high-accuracy Li-ion battery performance circuit model is yet to be established to cover all influential factors because of the diversity of Li-ion battery performance influences and their high nonlinearity.

REFERENCES

[1]   Q. Chen and C. Lin, *Automobile Technology*, **3**, 1 (2005).

[2]   C. Lin, B. Qiu, and Q. Chen, *Chinese Journal of Mechanical Engineering*, **12**, 76 (2005).

[3]   H. Dai, X. Wei, and Z. Sun, *Journal of Tongji University*, **1**, 98 (2010). [DOI: http://dx.doi.org/10.3969/j.issn.0253-374x.2010.01.018]

[4]   S. J. Lee, J. H. Kim, J. M. Lee, and B. H. Cho, *Journal of Power Sources*, **2**, 1367 (2008). [DOI: http://dx.doi.org/10.1016/j.jpowsour.2008.08.103].

[5]   C. Lin, B. Qiu, and Q. Chen, *Automotive Engineering*, **3**, 229 (2006). [DOI: http://dx.doi.org/10.3321/j.issn:1000-680X.2006.03.004]

[6]   A. Vasebi, M. Partovibakhsh, and S.M.T. Bathaee, *Journal of Power Sources*, **1**, 30 (2007). [DOI: http://dx.doi.org/10.1016/j.jpowsour.2007.04.011]

[7]   I. S. Kim and C. Ju, *IEEE Transactions on Power Eelectronics*, **4**, 2027 (2008). [DOI: http://dx.doi.org/10.1109/TPEL.2008.924629]

[8]   United States Idaho National Engineering & Environmental Laboratory, *Freedom CAR Battery Test Manual for Power-Assist Hybrid Electric Vehicles*, http://avt.inel.gov/battery/pdf/freedomcar_manual_04_15_03.pdf (2003).

[9]   X. Hu, S. Li, and H. Peng, *Journal of Power Sources*, **15**, 359 (2012). [DOI: http://dx.doi.org/10.1016/j.jpowsour.2011.10.013]

[10] A. Lasia, *Electrochemical Impedance Spectroscopy and its Applications* (Springer, New York, 2014) p. 217.

[11] J. M. Lee, O. Y. Nam, and B. H. Cho, *Journal of Power Sources*, **1**, 9 (2007). [DOI: http://dx.doi.org/10.1016/j.jpowsour.2007.03.072]

[12] W. Luo, C. Lv, L. Wang, and C. Liu, *Proc. the 6th IEEE Conference Industrial Electronics and Applications* (Beijing, China, 2011) p. 1943. [DOI: http://dx.doi.org/10.1109/ICIEA.2011.5975910]

[13] T. Huria, M. Ceraolo, J. Gazzarri, and R. Jackey, *Proc. IEEE International Electric Vehicle Conference 2012* (Greenville County, USA, 2012) p. 1. [DOI: http://dx.doi.org/10.1109/IEVC.2012.6183271]

[14] W. Gao, M. Jiang, and Y. Hou, *Proc. 6ᵗʰ IEEE Conference Industrial Electronics and Applications 2011* (Beijing, China, 2011) p. 2294. [DOI: http://dx.doi.org/10.1109/ICIEA.2011.5975974].

[15] J. Garcia and P. Areny, *Sensors and Actuators A: Physical*, **1**, 122 (2006). [DOI: 10.1016/j.sna.2006.04.014]

[16] M. Li, J. Zhang, and F. Zhang, *Automotive Engineering*, **6**, 554 (2006). [DOI: http://dx.doi.org/10.3321/j.issn:1000-680X.2006.06.011]

[17] T. Markel, A. Brooker, T. Hendricks, V. Johnson, K. Kelly, B. Kramer, M. O. Keefe, S. Sprik, and K. Wipke, *Journal of Power Sources*, **2**, 255 (2002). [DOI: http://dx.doi.org/10.1016/S0378-7753(02)00189-1]